

# Origin of $\pi$ -Facial Stereoselectivity of Nucleophilic Addition to Carbonyl Compounds. Application of the Exterior Frontier Orbital Extension Model to Cyclohexanones with Polar Substituent

Shuji Tomoda\* and Takatoshi Senju

Department of Life Sciences, Graduate School of Arts and Sciences,  
The University of Tokyo, Komaba, Meguro-ku, Tokyo 153-8902, Japan

Received 28 December 1998; accepted 29 January 1999

**Abstract:** The application of the exterior frontier orbital extension model (EFOE model) to  $\pi$ -facial stereoselection of cyclohexanones with a polar substituent at C3 or C4 have been described. The theoretical prediction that a linear correlation should exist between the  $\pi$ -facial (*axial* and *equatorial*) difference in the square of the EFOE densities ( $\lambda = \text{EFOE}(ax)^2 - \text{EFOE}(eq)^2$ ) and experimentally obtained facial selectivity ( $\ln(ax/eq)$ ) has been demonstrated for 5-substituted 2-decalones (**1**), 4-substituted cyclohexanones (**2**) and 3-substituted cyclohexanones (**3**). In addition, facial stereoselection of **3**, where the substituent is located closer to the reaction center compared with those of **1** or **2**, showed remarkable dependence on steric effects evaluated by the  $\pi$ -plane-divided accessible space (PDAS), another important quantity of the EFOE model, which represents simple summation of the  $\pi$ -plane-divided exterior three-dimensional space nearest to the reaction center outside the van der Waals surface of the substrate. © 1999 Elsevier Science Ltd. All rights reserved.

## INTRODUCTION

Since Cieplak's proposal of his conceptual model in 1981,<sup>1</sup> the origin of facial diastereoselection of addition reactions to unsaturated organic substrates has attracted considerable chemist's attention.<sup>2</sup> Most discussions are focused on the importance of transition state stabilization arising from the *anti*-periplanar hyperconjugative stabilization effect involving the incipient bond and/or from the torsional strain of substrate.<sup>3,4</sup> The distinction between the two opposite mechanisms of the *anti*-periplanar effect, known as the Felkin-Anh model<sup>4</sup> and the Cieplak model,<sup>1</sup> has been the subject of intense investigation (Figure 1).

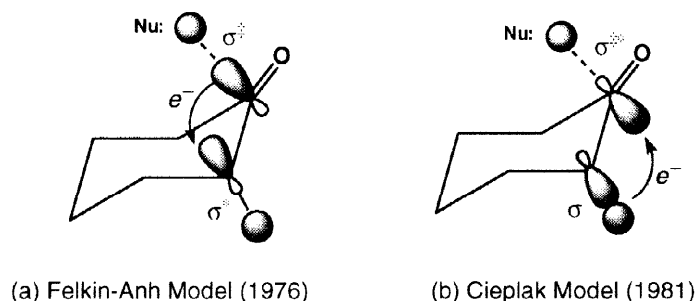
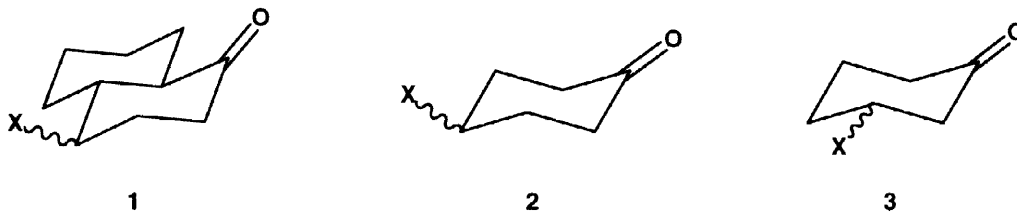


**Figure 1.** Mechanisms of *anti*-periplanar hyperconjugation effect in the axial transition state of cyclohexanone reduction.<sup>1-4</sup> (**Nu:** = nucleophile)

Recently we reported a quantitative analysis of the first transition states of carbonyl reduction with  $\text{LiAlH}_4$  using the natural bond orbital analysis<sup>5</sup> and proposed that the transition state effects, such as torsional strain and the *anti*-periplanar effect, are not essential for facial diastereoselection of nucleophilic additions to various cyclic ketones including 2-adamantanones.<sup>6</sup> It was found that the incipient bond is electron-deficient, showing the predominance of the Cieplak mechanism<sup>1</sup> over the Felkin-Anh mechanism.<sup>4</sup> Surprisingly the transition state effects often operate against observed facial stereoselectivity.

In the present paper, we describe the details of the exterior frontier orbital extension model (the EFOE model) previously proposed<sup>7,8</sup> as our new theoretical approach toward understanding  $\pi$ -facial stereoselection and its further application to 5-substituted *trans*-2-decalones (**1**)<sup>9</sup> and 4- or 3-substituted cyclohexanones (**2** and **3**), for which various controversial mechanisms of facial stereoselection have been proposed.



## RESULTS AND DISCUSSION

### Theoretical Description of the EFOE Model

The details of the definition of the two quantities of the EFOE model have been described elsewhere.<sup>7,8</sup> A brief description will be given here. The EFOE model focuses on the first and third terms of the Salem-Klopman equation (Eq. 1).<sup>10,11</sup>

$$\Delta E = \underbrace{-\sum_{ab} (q_a + q_b) \beta_{ab} S_{ab}}_{\text{1st term}} + \underbrace{\sum_{k < l} \frac{Q_k Q_l}{r_{kl}}}_{\text{2nd term}} + \underbrace{\sum_r^{\text{occ.}} \sum_s^{\text{unocc.}} - \sum_s^{\text{occ.}} \sum_r^{\text{unocc.}} \frac{2(\sum_{ab} c_{ra} c_{sl} \beta_{ab})^2}{E_r - E_s}}_{\text{3rd term}} \quad (1)$$

$q_a, q_b$  = electron populations in atomic orbital  $a$  or  $b$ .

$\beta$  = resonance integral,  $S$  = overlap integral

$Q_k, Q_l$  = total electron densities at atom  $k$  or  $l$ .

$r_{kl}$  = distance between atoms  $k$  and  $l$ .

$E_r$  = energy level of MO  $r$ .

$c$  = molecular orbital coefficients

The first term of Eq. 1 is the exchange repulsion term, which corresponds to the interactions among filled orbitals of the reactants. This term always leads to the destabilization of the system and is generally considered as steric effect in organic chemistry. The second term is the electrostatic interaction term that is especially important in ionic reactions. The third term is the donor-acceptor orbital interaction term, which should always leads to stabilization of the reacting system, and to which the frontier orbital interaction between reactants generally contributes most. Among these three terms, Salem and Klopman pointed out

that the first and the third terms should be particularly important in common organic reactions.

The EFOE model also focuses on the first and the third terms of this equation. It is designed for quantitative evaluation of these two terms to identify essential factors of  $\pi$ -facial stereoselectivity of addition reactions of  $\pi$ -systems in general including ketones, alkenes, and enolates etc. and eventually to predict  $\pi$ -facial stereoselectivity with some simple calculations and rules. Two new quantities –  $\pi$ -plane-divided accessible space (PDAS) as the steric effect term and the exterior frontier orbital extension density (EFOE density) as the orbital interaction term– constitute the new model. Both quantities focus on the exterior area of a molecule.

### 1. $\pi$ -Plane-Divided Accessible Space (PDAS)

A simple quantitative parameter of  $\pi$ -facial steric effect should provide convenient means to gain clearer and more effective perception in designing organic synthesis. Described below is the first method of  $\pi$ -facial steric effect calculation that is useful for common organic unsaturated substrates.

The new method focuses on three-dimensional space outside the van der Waals surface of a reactant molecule.<sup>12</sup> It is based on the simple assumption that the volume of the outer (exterior) space nearest to a reaction center should contain steric information of the reactant (substrate), since this volume is precisely the three-dimensional space available for a reagent to access the reaction center of the substrate. The exterior volume is calculated for two faces of  $\pi$ -plane separately. Figure 2 illustrates the definition of  $\pi$ -plane-divided accessible space (PDAS) as a reasonable quantitative measure of  $\pi$ -facial steric effect using formaldehyde as an example. Molecular surface is defined as an assembly of spherical atoms having the van der Waals radii.<sup>19</sup> Integration of exterior three-dimensional space for the PDAS of the carbonyl carbon is performed according to the following conditions. If a three-dimensional point  $P(x, y, z)$  outside the repulsive surface is the nearest to the surface of the carbonyl carbon (a reaction center on  $xz$  plane) (*i.e.* if the distance between  $P$  and the van der Waals surface of the carbonyl carbon ( $d_C$ ) is the shortest compared with the distances from  $P$  to other atomic surface (two  $d_H$  and one  $d_O$ ) ) and if the point is located above the carbonyl plane ( $y > 0$ ), the space at this point is assigned to the above-space of the carbonyl carbon. The integration (summation) of such points is defined as the PDAS of the carbonyl carbon for the above-plane. For the sake of convenience, spatial integration is limited to 5 au (2.65 Å) from molecular surface, where extension of an electronic wave function is negligible beyond this limit. In general, the carbonyl plane is defined as the plane which includes the two  $sp^2$  atoms of the  $\pi$ -bond and which is parallel with the vector connecting the two atoms at the  $\alpha$ -positions.

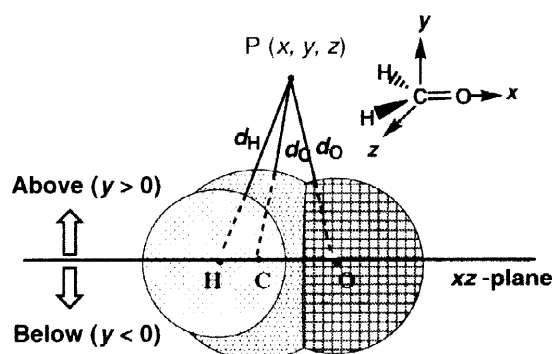


**Figure 2.** Definition of  $\pi$ -plane-divided accessible space (PDAS) for the case of formaldehyde.

## 2. Exterior Frontier Orbital Extension Density (EFOE Density)

The importance of the exterior area of a substrate in  $\pi$ -facial stereoselection has also been quantified by the definition of exterior frontier orbital extension density (EFOE density), which represents the third term of Eq. 1.<sup>10</sup> Thus the  $\pi$ -plane-divided EFOE density (hereafter called simply "EFOE density") is defined as the integrated (summed) electron density of a frontier orbital (FMO; the highest occupied molecular orbital; HOMO for electrophilic addition or the lowest unoccupied molecular orbital; LUMO for nucleophilic addition)<sup>14</sup> over specific exterior points over one face of the  $\pi$ -plane of a substrate molecule satisfying the following condition: *the absolute total value of the wave functions belonging to the carbonyl carbon makes a maximum contribution to the total value of FMO wave function at the point*. Such a condition guarantees that the driving force vector on hydride or other reagent is maximally directed toward the  $sp^2$  reaction center. Thus integration of FMO probability density ( $\Psi_{\text{FMO}}^2$ ) over such three-dimensional subspace ( $\Omega$ ) that satisfies the above condition should afford a reasonable quantitative measure of the third term of Eq. 1.<sup>10</sup> The values of EFOE density are expressed in % for the sake of numerical convenience by normalizing the wave function ( $\Psi_{\text{FMO}}$ ) to 100 (Eq. 2).

$$\text{EFOE density (\%)} = 100 \times \int \Psi_{\text{FMO}}^2 d\Omega \quad (2)$$

Based on the Salem and Klopman equation (Eq. 1)<sup>10</sup> and the second-order perturbation theory<sup>15</sup> at the extended Hückel level,<sup>16</sup> a simple linear correlation between the EFOE density and activation enthalpy ( $\Delta H^\ddagger$ ) can be derived assuming that EFOE density should be proportional to the overlap integral ( $S$ ) between reactant FMO's. One obtains the following equation, which describes the linear relation between  $\lambda$  ( $= \text{EFOE}(a)^2 - \text{EFOE}(a)^2$ ) and  $\Delta\Delta H^\ddagger$  (Eq. 3).

$$\therefore \Delta\Delta H^\ddagger = m\lambda + n \quad (m > 0; n : \text{a constant}) \quad (3)$$

For a graphical plot of Eq. 3, natural log of observed stereoselectivity (product ratio) may be used if experimental or calculated  $\Delta\Delta H^\ddagger$  is not available.

## Computational Methods

Spatial integration is limited to 5 au (2.65 Å) from molecular surface, where extension of an electronic wave function is negligible beyond this limit. The carbonyl plane is defined as the plane which includes both  $sp^2$  atoms of the  $\pi$ -bond (C=O) and which is parallel with the vector connecting the two carbon atoms at the  $\alpha$ -positions (C1 and C3). Bondi's van der Waals radii<sup>13</sup> were employed for the definition of molecular surface. The calculation procedure usually begins with structure optimization at the HF/6-31G(d) level using Gaussian 94 followed by a single point calculation with "gfinput" and "pop=full" keywords at the same level.<sup>17</sup> For bromides, Huzinaga's 43321/4321/311(d) basis was used for Br<sup>18</sup> with 6-31G(d) basis for C and H.

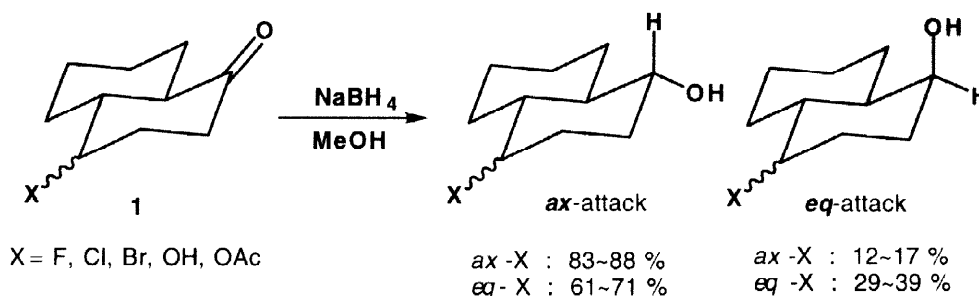
The computer program was designed so that simultaneous calculation of both PDAS and EFOE density could be performed according to the three-dimensional lattice method with a unit lattice volume of  $0.001 \sim 0.008 \text{ au}^3$  ( $1.48 \times 10^{-4} \sim 1.18 \times 10^{-3} \text{ Å}^3$ ). The quality of each EFOE calculation was checked by the value of the total electron density, which converged nearly unity ( $1.000 \pm 0.001$ ). All calculations were

carried out on a Silicon Graphics Power Indigo II or an IBM SP2 computer.

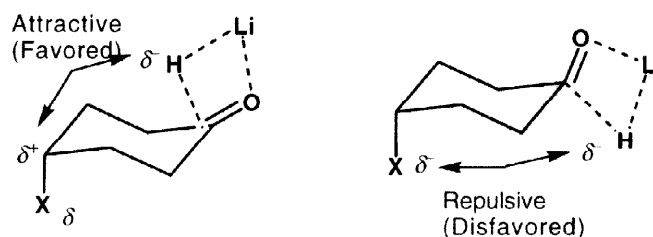
## Application of the EFOE Model

### 1. 5-Substituted *trans*-2-Decalones

In 1991, Houk reported an interesting observation on the facial selection of the  $\text{NaBH}_4$  reduction of the *trans*-2-decalone system (**1**) carrying a polar substituent (X) at C-5 (X = F, Cl, Br, OH, OAc).<sup>9</sup> A noteworthy feature on the stereochemistry of the product alcohol is the "axial effect": axial X prefers more axial attack (axial attack ; 83 - 88 %) than the corresponding equatorial X (axial attack ; 61 - 71 %).



Houk interpreted the axial effect in terms of electrostatic interactions between substituent and incoming hydride. An axial substituent would cause more electrostatic repulsive forces with the hydride undergoing attack from the equatorial face. An attractive electrostatic force may be expected for *ax*-attack on the substrate with axial substituent (Scheme 1). On the other hand, there would be no such repulsion for an equatorial substituent. This explanation was based on single-point transition state calculations at the HF/3-21G level performed by simple attachment of a substituent with a standard bond distance at the 4-position of the optimized LiH transition states of cyclohexanone. It was claimed that torsional strain should also be responsible for the axial effect.<sup>9</sup> Dannenberg explained the axial effect by his PPFMO method using the 4-substituted cyclohexanones as model compounds.<sup>19</sup> Cieplak assumed that the long-range interaction between the lone-pair of an axial substituent and the reaction center should lead to the extra-stabilization of the *anti*-periplanar incipient bond in the axial transition state.<sup>1</sup>



**Scheme 1.** Houk's electrostatic model to explain the axial effect.

The EFOE model analyses strongly indicate that the axial effect can be explicable with both frontier orbital extension and steric effects of the ground-state decalones (Table 1). It is obvious that the orbital distortion indices ( $\delta$ )<sup>8,20</sup> suggest no clear relationship with the observed stereochemistry. As seen in the axial values of PDAS in Table 1 (14 ~ 15 au<sup>3</sup>), the axial face of the 2-decalone system (**1**) is sterically much

more demanding (or sensitive to facial selection) than that of cyclohexanone (PDAS for the *ax*-face =  $\sim 19.4$  au<sup>3</sup>) owing to the additional cyclohexane ring fused in the former. In all cases examined, axial substituents tend to give larger EFOE density values in the *ax*-face than those in equatorial orientation. Such a trend seems enhanced for the substituents with lone pair inside the ring (OH and NH<sub>2</sub>), which give rise to the more stable conformations with greater axial PDAS values (15.3  $\sim$  15.5 au<sup>3</sup>) compared with the lone pair inside conformers (14.2  $\sim$  14.8 au<sup>3</sup>). Furthermore, in all cases of the three halogen substituents, the PDAS values for the substituents in the axial orientation are slightly larger in the *ax*-face (15.0, 15.7, 15.7 au<sup>3</sup> for F, Cl, Br, respectively) than those with the substituents in equatorial position (13.1, 15.0, 14.8 for F, Cl, Br, respectively). The equatorial values of the PDAS parameter for substituents Cl and Br are interesting in that they are reduced when Cl or Br is in axial position (46.6 $\rightarrow$ 45.8, 47.0 $\rightarrow$ 45.5 au<sup>3</sup> for Cl and Br, respectively), presumably due to skeletal deformation of the decalone system arising from significant 1,3-diaxial interaction of *ax*-Cl and *ax*-Br. On the other hand, the PDAS values for OH and NH<sub>2</sub> substituents make only marginal difference within the same lone pair conformations (14.2  $\sim$  14.8 au<sup>3</sup> for lone pair outside and 15.3  $\sim$  15.5 au<sup>3</sup> for lone pair inside conformations), indicating that these second-row substituents should not cause ring-deformation even when they are in axial orientation. Consequently, the steric effects induced by the orientation of Cl and Br substituents at the C5 position cannot be ignored in facial selection of the 2-decalone system.

**Table 1.** EFOE Analysis and Experimental Facial Selectivity of Hydride Reduction of 5-Substituted(X) 2-Decalones (**1**).<sup>a</sup>

X <sup>b</sup>	EFOE Density (%)		PDAS (au <sup>3</sup> )		$\delta$ (%) <sup>c</sup>	Obs. <sup>d</sup> <i>ax</i> : <i>eq</i>
	<i>ax</i>	<i>eq</i>	<i>ax</i>	<i>eq</i>		
H	1.708	0.343	14.5	47.3	48.2	60 : 40
<i>eq</i> -F	1.726	0.327	13.1	45.8	50.7	–
<i>ax</i> -F	1.955	0.458	15.0	47.6	49.9	87 : 13
<i>eq</i> -Cl	1.692	0.326	15.0	46.6	49.5	71 : 29
<i>ax</i> -Cl	1.711	0.440	15.7	45.8	52.6	88 : 12
<i>eq</i> -Br	1.686	0.340	14.8	47.0	48.9	66 : 34
<i>ax</i> -Br	1.991	0.300	15.7	45.5	51.5	–
<i>eq</i> -OH (lp-out)	1.730	0.379	14.6	47.4	50.6	61 : 39
<i>eq</i> -OH (lp-in)	1.618	0.307	15.4	46.2	49.7	–
<i>ax</i> -OH (lp-out)	1.671	0.241	14.2	47.6	47.2	85 : 15
<i>ax</i> -OH (lp-in)	1.911	0.353	15.3	46.8	49.9	85 : 15
<i>eq</i> -NH <sub>2</sub> (lp-out)	1.645	0.351	14.2	47.8	49.1	–
<i>eq</i> -NH <sub>2</sub> (lp-in)	1.622	0.306	15.5	45.8	48.7	–
<i>ax</i> -NH <sub>2</sub> (lp-out)	1.761	0.252	14.8	46.7	48.9	–
<i>ax</i> -NH <sub>2</sub> (lp-in)	1.956	0.232	15.5	46.1	51.9	–

<sup>a</sup> HF/6-31G(d). <sup>b</sup>lp-out = lone pair outside the ring; lp-in = lone pair inside the ring. <sup>c</sup>Orbital distortion index.<sup>20</sup> Positive value indicates distortion toward the *ax* direction. <sup>d</sup>NaBH<sub>4</sub>. Ref. 9.

It should be noted here that the EFOE density value for the axial face of a substrate with an *ax*-

substituent with lone pair inside for OH or NH<sub>2</sub> (1.955, 1.711, 1.991, 1.911, 1.956 for *ax*-F, Cl, Br, OH, NH<sub>2</sub>, respectively) is greater than the corresponding value for the axial face of a substrate with an *eq*-substituent with lone pair inside for OH or NH<sub>2</sub> (1.726, 1.692, 1.686, 1.618, 1.622 for *eq*-F, Cl, Br, OH, NH<sub>2</sub>, respectively). The importance of the frontier orbital extension in the decalone system has been more clearly indicated by the EFOE plot (Eq. 3) shown in Figure 3. A good linear correlation between  $\lambda$  ( $= \text{EFOE}(ax)^2 - \text{EFOE}(eq)^2$ ) and stereoselectivity ( $\ln(ax/eq)$ ) was obtained if *ax*-Cl is excluded ( $r^2 = 0.89$ ). The remarkable linear relationship can be considered as another strong evidence that the EFOE density values integrated over the exterior subspace  $\Omega$  (Eq.2) contain kinetic information of a reaction.

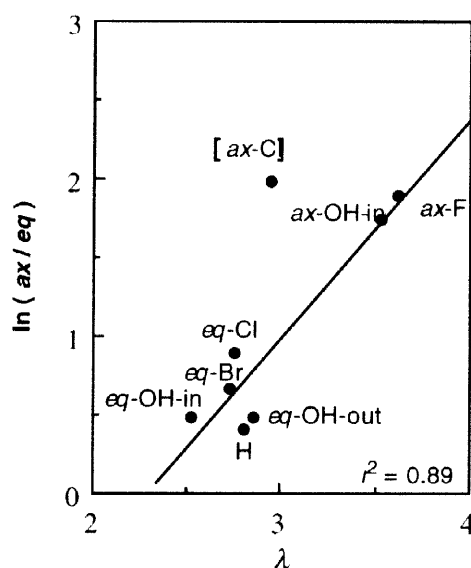


**Figure 3.** Plot of facial selectivity ( $\ln(ax/eq)$ ) vs.  $\lambda$  for 5-substituted *trans*-decalones (**1**). Least square analyses were performed excluding *ax*-Cl.

## 2. 4-Substituted Cyclohexanones

In connection with the facial stereoselection of the 5-substituted 2-decalones (**1**), the EFOE parameters of 4-substituted cyclohexanones (**2**) were calculated (Table 2). In contrast to **1**, the PDAS values for **2** do not suggest the above-mentioned substituent-induced ring-deformation effect in the cyclohexanone system for heavy halogen substituents (Cl, Br). Since experimental data for this system (**2**) were not available, the transition states of LiAlH<sub>4</sub> reduction were calculated at the HF/6-31+G(d) level. The calculated enthalpy differences of the transition states ( $\Delta\Delta H^\ddagger$ ) are also listed in the table. As shown in Figure 4, a remarkable linear correlation is again observed between  $\lambda$  values and  $\Delta\Delta H^\ddagger$  or the  $\ln(ax/eq)$  values for the decalone system if *ax*-Cl and *ax*-Br are excluded. The magnitude of  $\Delta\Delta H^\ddagger$  suggests that an *ax*-substituent uniformly prefers more *ax*-attack compared with an *eq*-substituent. The deviation of *ax*-Cl and *ax*-Br, as observed in the decalone system described above, may be attributed to the decreased extension of the local LUMO around the carbonyl carbon due to the significant remote in-phase mixing of the low-lying  $\sigma^*_{C-Cl}$  or  $\sigma^*_{C-Br}$  orbital, leading to inevitable reduction in the EFOE density values.

Hence the EFOE analyses provide strong evidence that the origin of the axial effect observed in the 5-substituted 2-decalones (**1**) can be rationalized with the ground-state properties of the substrates.

**Table 2.** EFOE Analysis and the Facial Difference in Activation Enthalpy ( $\Delta\Delta H^\ddagger$ ) for 4-Substituted(X) Cyclohexanones (**2**).<sup>a</sup>

$X^b$	EFOE Density (%)		PDAS (au <sup>3</sup> )		$\delta$ (%) <sup>c</sup>	$\Delta\Delta H^\ddagger$ <sup>d</sup>
	<i>ax</i>	<i>eq</i>	<i>ax</i>	<i>eq</i>		
H	1.940	0.249	19.4	47.2	55.1	1.61
<i>eq</i> -F	1.947	0.246	21.3	44.5	56.4	1.77
<i>ax</i> -F	2.151	0.359	20.1	47.3	55.7	2.35
<i>eq</i> -Cl	1.943	0.229	21.1	44.9	55.5	1.71
<i>ax</i> -Cl	1.824	0.333	20.4	45.5	58.3	2.46
<i>eq</i> -Br	1.861	0.255	20.8	45.2	57.1	1.86
<i>ax</i> -Br	1.894	0.224	20.2	45.5	53.5	2.57
<i>eq</i> -OH (lp-out)	1.916	0.289	19.7	46.7	56.3	–
<i>eq</i> -OH (lp-in)	1.862	0.230	21.3	44.5	55.4	1.67
<i>ax</i> -OH (lp-out)	1.961	0.184	18.7	47.7	54.3	–
<i>ax</i> -OH (lp-in)	2.077	0.275	20.0	46.6	55.6	2.26
<i>eq</i> -NH <sub>2</sub> (lp-out)	1.882	0.265	19.6	46.9	55.2	–
<i>eq</i> -NH <sub>2</sub> (lp-in)	1.823	0.217	21.5	44.2	54.4	1.66
<i>ax</i> -NH <sub>2</sub> (lp-out)	1.947	0.190	19.1	46.6	54.9	–
<i>ax</i> -NH <sub>2</sub> (lp-in)	2.026	0.248	20.6	45.4	51.9	2.12
<i>eq</i> -SiH <sub>3</sub>	0.959	0.399	14.4	55.5	19.3	–
<i>ax</i> -SiH <sub>3</sub>	0.785	0.345	14.1	54.5	30.0	–

<sup>a</sup> HF/6-31G(d). <sup>b</sup> lp-out = lone pair outside the ring; lp-in = lone pair inside the ring. <sup>c</sup> Orbital distortion index.<sup>20</sup> Positive value indicates distortion toward the *ax* direction. <sup>d</sup> Transition states of LiAlH<sub>4</sub> reduction calculated at the HF/6-31+G(d) level.  $\Delta\Delta H^\ddagger = H^\ddagger_{eq} - H^\ddagger_{ax}$ .

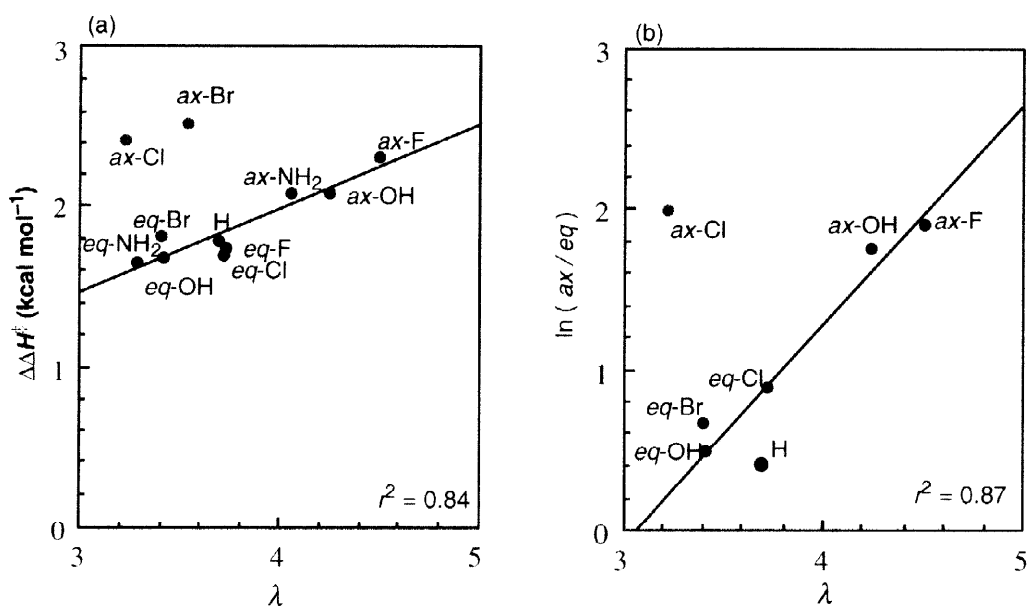


**Figure 4.** Plot of (a)  $\Delta\Delta H^\ddagger$  vs.  $\lambda$  and (b)  $\ln(ax/eq)$  vs.  $\lambda$  for 4-substituted cyclohexanones (**2**).  $\Delta\Delta H^\ddagger$  was calculated for LiAlH<sub>4</sub> reduction at the HF/6-31+G(d) level. Least square analyses were performed excluding *ax*-Cl and *ax*-Br.



### 3. 3-Substituted Cyclohexanones

Four controversial explanations have appeared to date to rationalize the enhancement of *ax*-attack in the cyclohexanone system carrying an electron-withdrawing substituent at the C3 position (the 3-substituent effect).<sup>21</sup> The Felkin-Anh model fails to give reasonable explanation.<sup>4</sup> The Cieplak model seems to predict correctly the observed stereochemistry by assuming diminished *anti*-periplanar hyperconjugative stabilization for *eq*-attack due to energy lowering of  $\sigma_{C2C3}$  orbital.<sup>1</sup> A good linear correlation was observed between product ratio ( $\ln(ax/eq)$ ) and  $\sigma_1$  values of the substituents at C3. He showed that the amount of *ax*-attack at the cyclohexanones with an electron-donating group at C3 (*t*-Bu, SiMe<sub>3</sub>) reduced slightly compared with parent cyclohexanone.<sup>21</sup> On the other hand, Mehta gave, in his 1992 paper, an alternative explanation based on steric relaxation over the *ax*-face due to slight pyramidalization of the carbonyl carbon in 3-fluorocyclohexanone.<sup>22</sup> Frenking has pointed out that enhanced frontier orbital (LUMO) extension over the axial face may be responsible.<sup>23</sup> On the other hand, Houk proposed possible importance of electrostatic interactions in systems with polar substituents in general.<sup>24</sup>

**Table 3.** EFOE Analysis and Observed Stereoselectivity of 3-Substituted(X) Cyclohexanones (3).<sup>a</sup>

X	EFOE Density (%)		PDAS (au <sup>3</sup> )		$\delta$ (%) <sup>b</sup>	Obs. (%) <sup>c</sup>	
	<i>ax</i>	<i>eq</i>	<i>ax</i>	<i>eq</i>		<i>ax</i>	<i>eq</i>
H <sup>d</sup>	1.799	0.249	19.6	46.7	52.8	21	79
<i>ax</i> -F	1.504	0.163	16.9	40.2	50.9	–	–
<i>eq</i> -F	2.070	0.283	21.6	45.6	54.0	–	–
<i>ax</i> -Cl	1.503	0.148	15.0	38.1	55.8	–	–
<i>eq</i> -Cl	1.865	0.221	20.6	45.5	47.1	–	–
<i>ax</i> -CF <sub>3</sub>	0.858	0.112	7.2	37.1	54.1	–	–
<i>eq</i> -CF <sub>3</sub>	1.998	0.320	19.9	45.7	50.9	50	50
<i>eq</i> -OMe	2.000	0.298	20.3	46.4	52.3	–	–
<i>ax</i> -Me	1.447	0.211	7.9	48.4	52.5	–	–
<i>eq</i> -Me	1.884	0.304	18.4	47.8	47.9	–	–
<i>eq</i> - <i>t</i> -Bu	1.820	0.316	17.3	47.3	49.6	19	81
<i>ax</i> -SiH <sub>3</sub>	0.999	0.127	7.6	48.2	50.0	–	–
<i>eq</i> -SiH <sub>3</sub>	0.803	0.116	17.6	48.6	34.7	–	–
<i>ax</i> -SiMe <sub>3</sub>	1.357	0.208	3.5	46.9	53.1	–	–
<i>eq</i> -SiMe <sub>3</sub>	1.709	0.291	16.9	49.0	49.1	15	85
<i>eq</i> -Ph	1.684	0.221	17.6	48.0	59.4	25	75
<i>eq</i> -C <sub>6</sub> H <sub>4</sub> - <i>p</i> -Me	1.614	0.206	17.6	48.0	59.1	23	77
<i>eq</i> -C <sub>6</sub> H <sub>4</sub> - <i>p</i> -OMe	1.289	0.129	17.4	48.1	67.7	24	76
<i>eq</i> -C <sub>6</sub> H <sub>4</sub> - <i>p</i> -CF <sub>3</sub>	1.829	0.265	17.8	48.0	54.4	28	72
<i>eq</i> -C <sub>6</sub> F <sub>5</sub>	1.849	0.251	18.6	46.3	58.6	34	66

<sup>a</sup> HF/6-31G(d). <sup>b</sup> Orbital distortion index. Positive value indicates distortion toward the *axial* direction.<sup>20</sup> <sup>c</sup> Reaction with MeLi in ether. Ref. 21a. <sup>d</sup> 4-*t*-Butylcyclohexanone.

The EFOE analyses provides strong theoretical evidence that the origin of the 3-substituent effect may exist again in the ground-state ketone substrates. Two notable features are seen in Table 3. First, compared with the data of parent cyclohexanone (X = H), the axial EFOE values for the *eq*-substituents

(2.070 (F), 1.998 (CF<sub>3</sub>), 2.000 (OMe) %) are greater than that of parent cyclohexanone (1.940 (H) %) except for Cl, Me and *t*-Bu in agreement with Frenking's explanation.<sup>23</sup> Similarly, in consonant with Mehta's suggestion, the axial PDAS values for *eq*-substituents (21.6(F), 20.6(Cl), 19.9 (CF<sub>3</sub>), 20.3 (OMe) au<sup>3</sup>) are larger than that of cyclohexanone (19.4 au<sup>3</sup>), whereas those for the electron-donating *eq*-substituents (18.4 (Me), 17.3 (*t*-Bu), 17.3 (SiH<sub>3</sub>), 16.9 (SiMe<sub>3</sub>) au<sup>3</sup>) are smaller than that of cyclohexanone. The two effects (PDAS and EFOE density) operating in the same direction for *ax*-attack preference in the ground-state 3-substituted cyclohexanones (**3**) are consistent with the experimental observations.<sup>21</sup> Table 4 collects the results of EFOE analysis on 3,5-*eq,eq*-disubstituted cyclohexanones (**4**). It is more clearly seen that the tendencies observed for **3** are enhanced in **4**: both PDAS values and EFOE densities for the *ax*-face are considerably reduced for **4** carrying electron-donating substituents. The two structural parameters in Table 4 indicate that the increase of PDAS values may be caused by the increment of the distance between C1 and the axial hydrogen at C3 ( $d_{\text{C1} \cdots \text{H3ax}}$ ) arising from ring deformation as seen in the change of the torsion angle between C=O and C2–C3(C5–C6) ( $\tau$ ).

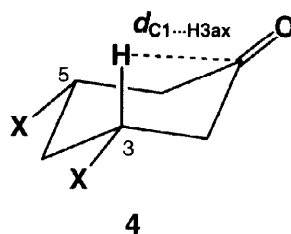


**Table 4.** EFOE Analysis of 3,5-*eq,eq*-Disubstituted(X) Cyclohexanones (**4**).<sup>a</sup>

X	EFOE Density (%)		PDAS (au <sup>3</sup> )		$\delta$ (%) <sup>b</sup>	$d_{\text{C1} \cdots \text{H3ax}}$ (Å)	$\tau$ (°) <sup>c</sup>
	<i>ax</i>	<i>eq</i>	<i>ax</i>	<i>eq</i>			
H	1.940	0.249	19.4	47.2	55.1	2.835	131.5
F	2.236	0.313	24.0	44.3	52.8	2.867	135.0
CF <sub>3</sub>	2.026	0.400	20.4	44.4	48.1	2.820	133.0
Cl	1.904	0.174	21.4	44.2	36.5	2.831	133.7
NH <sub>3</sub> <sup>+</sup>	1.487	0.156	19.5	46.2	43.6	2.833	131.9
Me	1.828	0.342	17.7	48.0	47.9	2.792	130.6
O <sup>−</sup>	1.604	0.704	12.2	61.8	27.4	2.757	124.4
SiH <sub>3</sub>	1.223	0.788	15.9	49.9	24.3	2.784	128.7
SiMe <sub>3</sub>	1.498	0.317	14.8	51.0	44.3	2.766	127.8

<sup>a</sup> HF/6-31G(d). <sup>b</sup> Orbital distortion index. Positive value indicates distortion toward the *axial* direction.<sup>20</sup> <sup>c</sup> Torsion angle between C=O and C2–C3(C5–C6).

Exactly the same trend is observed for the five aryl-substituted cases listed in Table 3. Figure 5(a) depicts a plot of  $\lambda$  against the natural log of product ratio ( $\ln(ax/eq)$ ) of MeLi addition in ether reported by Cieplak.<sup>21</sup> Two approximately linear correlations – one for four cases of aliphatic substituents and the other for five cases of aromatic ones – may be another strong theoretical evidence for the importance of frontier orbital extension over the exterior of substrate ketones as the origin of  $\pi$ -facial stereoselection. Furthermore, a plot of PDAS values for the *ax*-face against stereoselection ( $\ln(ax/eq)$ ) (Figure 5(b)) exhibits remarkable linear correlation if X = H (*eq-t*-butylcyclohexanone) is excluded. Again, it is not

necessary to assume the role of neither transition state hyperconjugative stabilization nor the electrostatic effects to explain the facial stereoselection observed for **3**. Ground-state conformational changes of cyclohexanone moiety caused by these substituents are most likely to be responsible for the observed trend of facial selection in **3**.

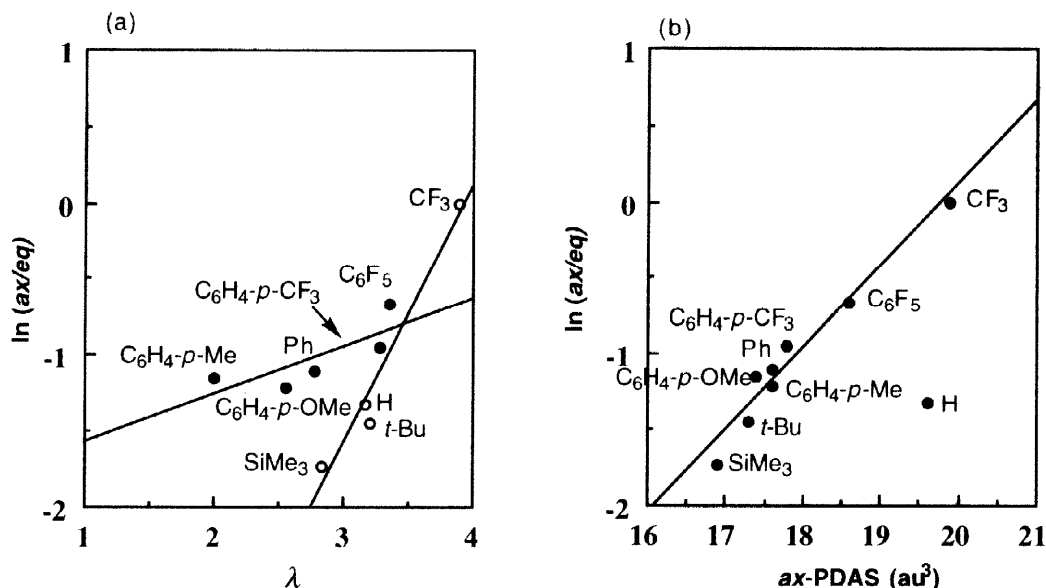


**Figure 5.** Plot of (a) facial selectivity ( $\ln(ax/eq)$ ) vs.  $\lambda$  (Open circles: aliphatic substituents ( $r^2 = 0.96$ ); Filled circles: aromatic substituents ( $r^2 = 0.63$ )) and (b) facial selectivity ( $\ln(ax/eq)$ ) vs. PDAS values for the  $ax$ -face of 3-substituted cyclohexanones (**3**) ( $r^2 = 0.95$  excluding  $X = H$ ;  $eq$ -4-*t*-butylcyclohexanone).

## CONCLUSIONS

The EFOE analysis strongly indicated that both "the axial effect" of 4-substituted cyclohexanones (**2**) and "the 3-substituent effect" of 3-substituted cyclohexanones (**3**) could be reasonably explained by the ground-state factors – the extension of LUMO and the molecular conformation – without invoking other influences, such as transition state effects,<sup>21</sup> remote lone pair participation,<sup>1</sup> or the electrostatic interaction effects.<sup>9</sup> The results presented here again provide strong theoretical evidence that the origin of subtle changes in  $\pi$ -facial selection may most probably exist in the ground-state conformation of substrates.

We have demonstrated the utility of the EFOE model so far on the cyclohexanone system<sup>6,8</sup> and the adamantanone system.<sup>6,7</sup> Our preliminary calculations have indicated that the approach should be applicable not only to other nucleophilic additions including Mehta's polycyclic systems,<sup>25</sup> but also to electrophilic additions of alkenes and lithium enolates. The results of these cases will be reported in due course.

## Acknowledgements:

The authors express our gratitude to Dr. M. Iwaoka for computational assistance. We thank the Ministry of Education, Culture and Sports for financial support through Grant-in-Aid for Scientific Research (Project Nos. 09440215 and 09239207).

## References and Notes

1. Cieplak, A. S. *J. Am. Chem. Soc.* **1981**, 103, 4540.
2. Gung, B. W. *Tetrahedron* **1996**, 52, 5263.
3. Wu, Y. D.; Houk, K. N. *J. Am. Chem. Soc.* **1987**, 109, 908.
4. (a) Chérest, M.; Felkin, H. *Tetrahedron Lett.* **1968**, 2205. (b) Chérest, M.; Felkin, H.; Prudent, N. *Tetrahedron Lett.* **1968**, 2199. (c) Anh, N. T.; Eisenstein, O.; Lefour, J. -M.; Tran Huu Dau, M. E. *J. Am. Chem. Soc.* **1976**, 95, 6146. (d) Anh, N. T.; Eisenstein, O. *Nouv. J. Chim.* **1976**, 1, 61.
5. (a) Reed, A. E.; Curtiss, L. A.; Weinhold, F. *Chem. Rev.* **1988**, 88, 899. (b) Glendening, E. D.; Weinhold, F. "Natural Resonance Theory I. General Formalism" in Technical Report of Theoretical Chemistry Institute. **1994**, No. 803.
6. Tomoda, S.; Senju, T. *Chem. Commun.* **1999** in press.
7. Tomoda, S.; Senju, T. Submitted.
8. Tomoda, S.; Senju, T. *Tetrahedron* **1997**, 53, 9057.
9. Wu, Y. -D.; Tucker, A.; Houk, K. N. *J. Am. Chem. Soc.* **1991**, 113, 5018.
10. (a) Klopman, G. *J. Am. Chem. Soc.* **1968**, 90, 223. (b) Salem, L. *ibid*, **1968**, 90, 543.
11. Fleming, I. *Frontier Orbitals and Organic Chemical Reactions*; John Wiley & Sons: London, 1977.
12. Ohno, K.; Matsumoto, S.; Harada, Y. *J. Chem. Phys.* **1984**, 81, 4447.
13. Bondi, A. *J. Phys. Chem.* **1964**, 68, 441.
14. Fukui, K. *Theory of Orientation and Stereoselection*; Springer Verlag: Heidelberg, 1979.
15. (a) Imamura, A. *Mol. Phys.* **1968**, 15, 225–238. (b) Libit, L.; Hoffmann, R. *J. Am. Chem. Soc.* **1974**, 96, 1370.
16. Hoffmann, R. *J. Chem. Phys.* **1963**, 39, 1397.
17. Gaussian 94 (Revision E.2); Gaussian, Inc., Pittsburgh, PA, 1997.
18. Huzinaga, S.; *Gaussian Basis Sets for Molecular Orbital Calculations*; Elsevier: Amsterdam, 1984.
19. (a) Huang, X. L.; Dannenberg, J. J.; Duran, M.; Bertran, J. *J. Am. Chem. Soc.* **1993**, 115, 4024. (b) Huang, X. L.; Dannenberg, J. J. *ibid*, **1993**, 115, 6017.
20. Orbital distortion index ( $\delta$ ) at carbonyl carbon (C-1) for the LUMO is defined by the following equation;  $\delta = 100 \times (d_A - d_E) / (d_A + d_E)$ , where  $d_A$  and  $d_E$  represent integrated "electron densities" due to the carbonyl carbon wave functions of the LUMO for both sides (axial and equatorial region) of the carbonyl plane.<sup>8</sup>
21. (a) C. R. Johnson, B. D. Tait A. S. Cieplak, *J. Am. Chem. Soc.* **1987**, 109, 5875. (b) Cieplak, A. S.; Tait, B. D.; Johnson, C. R. *J. Am. Chem. Soc.* **1989**, 111, 8447.
22. Amarendra, Y.; Yenkatesan, K.; Ganguly, B.; Chandrasekhar, J.; Khan, F. A.; Mehta, G. *Tetrahedron Lett.* **1992**, 33, 3072.
23. Frenking, G.; Kohler, K. F.; Recz, M. T. *Angew. Chem. Int. Ed. Engl.* **1991**, 30, 1146.
24. Wu, Y.-D.; Houk, K. N.; Padden-Row, M. N. *Angew. Chem. Internat. Ed.* **1992**, 31, 1019.
25. (a) Ganguly, B.; Chandrasekhar, J.; Khan, F. A.; Mehta, G. *J. Org. Chem.* **1993**, 58, 1734. (b) Mehta, G., Khan, F. A. *J. Chem. Soc. Chem. Commun.* **1991**, 18. (c) Mehta, G., Khan, F. A. *J. Am. Chem. Soc.* **1990**, 112, 6140. (d) Mehta, G., Khan, F. A.; Gadre, S. R.; Shirsat, R. N.; Ganguly, B.; Chandrasekhar, J. *Angew. Chem. Internat. Ed.* **1994**, 33, 1390.